

# FIXED ORDER PQ-CONTROL DESIGN METHOD FOR DUAL-STAGE INSTRUMENTED SUSPENSION

M. Graham\* R.J.M. Oosterbosch\*\*  
R.A. de Callafon\*<sup>1</sup>

\* *University of California, San Diego, Dept. of Mechanical  
and Aerospace Engineering, 9500 Gilman Drive, La Jolla,  
CA 92093-0411, U.S.A*

\*\* *Eindhoven University of Technology, Dept. of  
Mechanical Engineering, 5600 MB Eindhoven, The  
Netherlands*

Abstract: To achieve frequency separation between actuators of a dual-stage servo actuator system in a hard disk drive, the PQ control design method can be used. In the PQ method, the servo controller is designed by focusing on structural interference of the actuators. This paper provides a specific parametrization for fixed order feedback controllers used in the PQ-method for which the structural interference between actuators can be minimized. The proposed control design method is applied to a dual-stage instrumented suspension, where the additional sensor of the instrumented suspension is used to attenuate high frequency disturbance caused by windage turbulence in a hard disk drive. *Copyright © 2005 IFAC.*

Keywords: Periodic; Disturbance Rejection; Servo Systems; Hard Disk Drive

## 1. INTRODUCTION

As data storage capacity of magnetic hard disk drive (HDD) systems increase, the requirements on the servo system become more challenging. Progress in areal storage density of a HDD can be accomplished by using a dual-stage actuator system, in which a high-bandwidth and highly accurate micro-actuator (MA) is used in combination with a traditional Voice Coil Motor (VCM) to perform the read/write tasks over the data track (Li and Horowitz, 2002; Li et al., 2003; Teerhuis et al., 2003). The use of dual-stage actuator systems has received great attention from the servo design community and an overview of the literature can for example be found in (Mamun et al., 2003). The driving force behind dual-stage servo control

design is to increase the bandwidth of the system for better disturbance rejection, while maintaining a trade-off for large AC squeezed written servo patterns on a magnetic disk.

In the dual-stage actuator system, the VCM and MA act in parallel, possibly causing structural interference of the actuators. Interference of dual-stage actuators can be avoided by providing frequency separation in an (optimal) control design (Rotunno and de Callafon, 2003) or explicitly placing the closed-loop zeros that are introduced due to the non-square input/output dimension of the dual-stage system. One control design technique that uses closed-loop zero placement to account for the dual-input single-output dynamic coupling, is the PQ-method proposed in (Schroeck et al., March 2001).

Although the PQ-method provides a framework to design low order controllers, no explicit paramet-

---

<sup>1</sup> Corresponding author. Tel.: +1.858-5343166; Fax: +1.858-8223107

ization of the feedback controller has been proposed. Furthermore, high bandwidth servo control in hard disk drives requires fast sampling of the position error signal (PES) and, in most drives, sampling frequencies of the PES are limited to approximately 20kHz. For high bandwidth digital control, an additional sensor instrumented on the suspension can provide high frequency measurements of suspension vibrations. The instrumented suspension signal (ISS) can be used to design a high bandwidth instrumented suspension inner-loop controller that dampens the resonance modes of the suspension (Li and Horowitz, 2002) or reduces high frequency vibrations due to windage (Vestmoen Nilsen and de Callafon, 2004).

This paper provides an explicit parametrization for the controllers used in the PQ-method and allows for an intuitive design of the dual-stage controller. Moreover, the parametrization is exploited to formalize the design of a dual-stage controller for a inner-loop controlled instrumented suspension. This allows for a design of the PQ-based dual-stage outer-loop servo controller in which the ISS is used for an inner-loop control of the suspension to reduce high frequency vibrations.

## 2. PQ-METHOD FOR DUAL-STAGE SERVO

### 2.1 General PQ Method Framework

The dual-stage servomechanism pictured in Figure 1 has two small motion piezoelectric (PZT) push-pull actuators located between the head suspension and the E-block. The E-block and the additional MA are moved by the rotary actuation of the VCM, making the motion of the two actuators act in parallel to follow a desired data circular track on the disk.



Fig. 1. Dual-Stage Suspension Disk Drive with Hutchinson Magnum 5E PZT dual-stage actuator

This servomechanism can be modeled by the dual-input single-output (DISO) closed loop system shown in Figure 2, where  $P_{ma}$  denotes the dynamic model of the micro-actuator (MA) and  $P_{vcm}$  is used to denote the dynamics of the voice-coil motor (VCM). For servo control design purposes, only the PES of the read/write head is fed back to the feedback controllers of the respective actuators.

The PQ-method (Schroek et al., March 2001) uses two steps to reduce the task of designing a

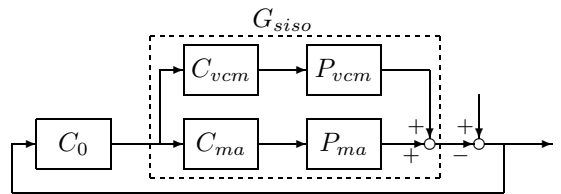


Fig. 2. Block diagram of servo controlled dual-stage suspension system

controller for a DISO system into two standard single-input single-output (SISO) control design problems. In the first step the zeros of the closed-loop system are placed using loop shaping or root locus techniques to address the structural interference between actuators. This design step is followed by a conventional feedback control design to achieve certain bandwidth requirements.

The possibility to place zeros can be seen by recognizing that the closed-loop zeros of the dual-stage feedback system depicted in Figure 2 are given by the zeros of  $C_0$  and  $G_{siso}$ , where

$$G_{siso}(s) := P_{ma}(s)C_{ma}(s) + P_{vcm}(s)C_{vcm}(s) \quad (1)$$

Clearly, structural interference of the actuators occurs at the zeros of  $G_{siso}$  and the zeros are equivalent to the closed-loop poles of the feedback connection of  $P$  and  $Q$ , where

$$P(s) = \frac{P_{vcm}(s)}{P_{ma}(s)} \quad \text{and} \quad Q(s) = \frac{C_{vcm}(s)}{C_{ma}(s)} \quad (2)$$

are defined respectively as the ratio of the individual actuator dynamics and the individual servo controller dynamics. The role of the first step in the PQ-method is to address the interference between the VCM and the MA by placing the zeros of the SISO system  $G_{siso}$  via an equivalent feedback control problem involving  $P$  and  $Q$  in (2). Since the control design in the first step uses the ratio of VCM and MA controllers, any common component of these controllers will cancel out in  $Q$ . The second step in the PQ-method is designing the overall (common) controller  $C_0$  for the feedback connection of  $G_{siso}$  and  $C_0$  depicted in Figure 2.

### 2.2 Explicit Q-Parametrization

As mentioned, the first step of the PQ-method is designing the controller  $Q(s)$  to stabilize the feedback connection of  $P$  and  $Q$ . Placement of the closed-loop poles of the feedback connection of  $P$  and  $Q$  ensures that  $G_{siso}$  has stable (closed-loop) zeros (Schroek et al., March 2001). The structural interference of the actuators can be eliminated completely, in case  $Q(s)$  is allowed to have the same (full) order as  $P(s)$ . In that case, standard observer and pole placement techniques can be used to design  $Q(s)$  to place closed-loop zeros at an arbitrary location (Franklin et al., 2002).

The design freedom for  $Q(s)$  can be parameterized by considering the minimum requirements on the controllers  $C_{vcm}$  and  $C_{ma}$  to achieve closed-loop stability; reduction of low frequency or steady-state disturbances; and frequency separation between the actuators to avoid structural interference. In order to characterize the desired design freedom in  $Q(s)$ , we first assume simplified models of the VCM  $P_{vcm}$  and MA  $P_{ma}$  given by

$$\begin{aligned} P_{vcm}(s) &= \frac{K_{vcm}\omega_1^2}{s^2(s^2 + 2\beta_1\omega_1s + \omega_1^2)} \\ P_{ma}(s) &= \frac{K_{ma}\omega_2^2}{s^2 + 2\beta_2\omega_2s + \omega_2^2} \end{aligned} \quad (3)$$

where  $\omega_1, \omega_2$  indicate the first or smallest resonance mode with damping ratio  $\beta_1, \beta_2$  found respectively in the VCM and MA dynamics. In (3) the dynamics of the VCM reflect a flexible structure with a single resonance mode, augmented with a double integrator to model the free-body motion of the rotary actuator. A similar model is used for the MA, exhibiting a different resonance mode, but without the free-body motion. As a result of (2) parameterized by (3), the minimal design freedom in  $Q(s)$  required to create a stable feedback connection of  $P$  and  $Q$  is given by

$$Q(s) = K \frac{\tau_1s + 1}{\tau_2s + 1}, \quad K > 0, \tau_1 > \tau_2 > 0 \quad (4)$$

specifying the design freedom of a straightforward lead-compensator. Typically, the smallest resonance mode  $\omega_2$  of the MA is larger than the smallest resonance mode  $\omega_1$  of the VCM and additional upper bounds on  $K, \tau_1$  and  $\tau_2$  are imposed to satisfy stability requirements.

Although (4) parameterizes the minimum design freedom to find a stable feedback connection of  $P$  and  $Q$  in the first step of the PQ-method, the choice of  $Q(s)$  limits the design freedom in  $C_{vcm}(s)$  and  $C_{ma}(s)$  to

$$C_{vcm}(s) = K \frac{\tau_1s + 1}{\tau_2s + 1}, \quad C_{ma}(s) = 1 \quad (5)$$

as both  $C_{vcm}(s)$  and  $C_{ma}(s)$  are required to be strictly proper. With the (trivial) choice in (5), no frequency separation between the dual-stage controllers is obtained as the MA controller  $C_{ma}$  is required to work over the whole frequency range.

In order to accommodate frequency separation and address the requirement of eliminating steady state force disturbances due to flex cable stiffness or friction forces in the actuator, the transfer function for the VCM controller  $C_{vcm}$  should contain an integrator. Further frequency separation between the actuators can be accomplished by requiring a high pass filter in the transfer function for the MA controller  $C_{ma}$  to focus the MA control energy at higher frequencies. With these design considerations and the minimal design freedom in

$Q(s)$  given in (4), the controllers  $C_{vcm}$  and  $C_{ma}$  are parameterized by

$$C_{vcm} = K \frac{\tau_d s + 1}{s} \frac{\tau_1 s + 1}{\tau_2 s + 1}, \quad C_{ma} = \frac{s}{\tau_d s + 1} \quad (6)$$

The design freedom of  $\tau_d$  determines the frequency at which the separation between the VCM and MA occurs. Variables  $\tau_1$  and  $\tau_2$  determine the lead-compensator parameters of the VCM. Given the controllers  $C_{vcm}$  and  $C_{ma}$  in (6), the transfer  $Q$  in (2) is explicitly parameterized by

$$\begin{aligned} Q(s) &= K \left( \frac{\tau_d s + 1}{s} \right)^2 \frac{\tau_1 s + 1}{\tau_2 s + 1}, \\ K > 0, \tau_d > 0, \tau_1 > \tau_2 > 0 \end{aligned} \quad (7)$$

With this parametrization and the choice for  $C_{vcm}$  and  $C_{ma}$  in (6), the control of the VCM actuator motion is dominant at frequencies below the crossover frequency whereas the MA motion contributes more at higher frequencies. The relative damping of the closed-loop poles of the feedback connection of  $P$  and  $Q$  determines the amount of destructive interference between the two actuators and can be measured by the phase- and amplitude-margin of the feedback connection of  $P$  and  $Q$  (Mamun et al., 2003).

### 2.3 Common controller parametrization

The second step of the PQ-method considers the design of the (common) controller  $C_0(s)$ , which establishes the overall performance of the dual-stage closed-loop system as indicated in Figure 2. For the parametrization of the controller  $C_0(s)$ , we can consider the feedback connection of  $C_0$  and  $G_{siso}$  defined in (1). Additional robustness to unmodeled resonance modes that might occur in the models  $P_{vcm}$  and  $P_{ma}$  can be provided by high frequency roll-off of the common controller. Limiting the complexity of the overall dual-stage controller, the second order transfer function

$$\begin{aligned} C_0(s) &= K_0 \frac{\omega_0^2}{s^2 + 2\beta_0\omega_0s + \omega_0^2} \\ K_0 > 0, \beta_0 > 0, \omega_0 > 0 \end{aligned} \quad (8)$$

is used for the parametrization of the common controller  $C_0(s)$ . The design freedom in  $C_0$  in the form of the scaling  $K_0$ , the cut-off frequency  $\omega_0$  and damping ration  $\beta_0$  can provide gain and phase margins for stability of the overall system.

## 3. PQ METHOD WITH INSTRUMENTED SUSPENSION MICRO-ACTUATOR

### 3.1 Controller configuration

Additional high frequency vibrations caused by windage disturbances can be monitored with an

instrumented dual-stage suspension. Such a configuration provides an instrumented suspension signal (ISS) that can be sampled at higher frequencies for control purposes.

For comparison purposes of the results presented in this paper, the same Hutchinson Magnum 5e suspension depicted in Figure 1 is used to generate an ISS. For that purpose, one piezoelectric element in the push-pull configuration of the MA is used to provide the ISS, while the other piezoelectric element is still used for push-pull actuation of the MA. The dynamic model  $P_{ma}$  of the MA must be distinguished from the dynamics of the instrumented suspension by  $P_{ima}$ . The dynamic model of the piezoelectric input signal  $u(t)$  to the ISS  $x(t)$  is denoted by  $P_{is}$ .

To separate the high sampling control on the basis of the ISS from the slow sampling control on the basis of the PES, a separate control design  $C_i$  is used for the control of the instrumented suspension. The controller configuration has been depicted in Figure 3, where both the instrumented suspension inner-loop controller  $C_i$  and the outer-loop dual-stage have been given.

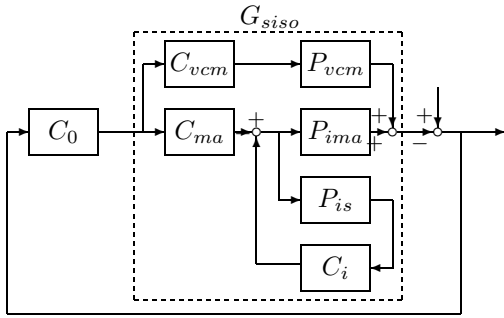


Fig. 3. Instrumented Suspension Disc Drive Block Diagram

From Figure 3 it can be seen that the inner-loop controller  $C_i$  modifies the open-loop dynamics of the instrumented MA  $P_{ima}$  to the controlled inner-loop dynamics  $\frac{P_{ima}}{1+C_i P_i}$  which serves as a new model for the MA dynamics. The instrumented controller  $C_i$  can be designed to dampen the resonance modes of the suspension (Li and Horowitz, 2002) or reduce high frequency vibrations due to windage (Vestmoen Nilsen and de Callafon, 2004; Li et al., 2003). The separation of the inner-loop controller  $C_i$  and the outer-loop controller allows for a straightforward extension of the PQ-method to design the dual-stage controller.

### 3.2 PQ-method for instrumented suspension

The flexibility of the PQ-method framework allows the inner feedback loop of  $C_i$  and  $P_{ima}$  to be incorporated into the design of outer-loop dual-stage controllers  $C_{vcm}$  and  $C_{ma}$ . With inner-loop control, the transfer function of  $P(s)$  is given by

$$P(s) = \frac{P_{vcm}(s)}{P_{ma}(s)}, \quad P_{ma}(s) := \frac{P_{ima}(s)}{1 + C_i(s)P_i(s)} \quad (9)$$

where  $P_{ma}$  is now the closed loop transfer function that provides active damping of the dual-stage suspension via the inner-loop control.

The inner-loop controller will alter the dynamics of the MA, but the basic dynamic behavior of  $P_{ma}$  in (9) will be similar to (3). As a result, the same parametrization for  $Q$  given in (7) and  $C_0$  given in (8) can be used.

## 4. APPLICATION OF CONTROL PARAMETRIZATION IN PQ METHOD

### 4.1 Models of Dual-Stage Suspension

The PQ-design of a dual-stage controller, using the parametrization of  $Q$  in (7) and  $C_0$  in (8), is illustrated using experimentally obtained models of the Hutchinson Magnum 5E piezoelectric MA mounted on a E-block of a VCM rotary actuator in an open HDD. Standard prediction error techniques were used to model the dynamics of the system shown in Figure 3 which includes the effects of windage on the dual stage suspension (Ljung, 1999; Suthasun et al., 2004). For reference purposes, the Bode plot of the identified models of the VCM ( $P_{vcm}$ ) and MA ( $P_{ma}$ ) with flexibilities of the E-block and dual-stage suspension are presented in Figure 4.

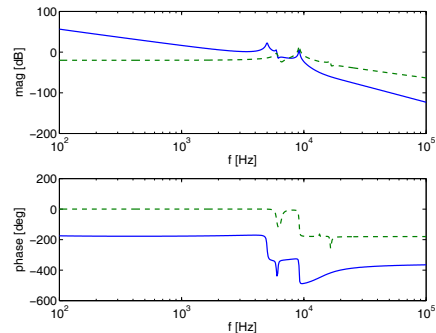


Fig. 4. Amplitude and phase Bode plot of 8th order VCM model  $P_{vcm}$  (solid) and 8th order MA model  $P_{ma}$  (dashed)

Both the models for  $P_{vcm}$  and  $P_{ma}$  are 8th order continuous time models and are more complex than (3), but they follow the basic pattern. The model  $P_{vcm}$  contains a double integrator and has a first resonance mode  $\omega_1 \approx 3.1 \cdot 10^4$  rad/s with a damping ratio of  $\beta_1 \approx 0.0125$ . The model  $P_{ma}$  of the MA exhibits its first resonance mode  $\omega_2 \approx 3.7 \cdot 10^4$  rad/s with a damping ratio of  $\beta_2 \approx 0.0205$ . However, both  $P_{vcm}$  and  $P_{ma}$  have additional resonance modes due to a strong sway mode of the suspension at approximately 9 kHz.

### 4.2 Dual-Stage Suspension Control Design

For the first step in the PQ-method, the design freedom of  $K > 0$ ,  $\tau_d > 0$ ,  $\tau_1 > \tau_2 > 0$  in (7) are explored using a root-locus method. Since

the poles of the feedback connection of  $P$  and  $Q$  are the zeros of  $G_{siso}$ , the poles are placed as far as possible into the left half plane in order to provide minimal structural interference of the VCM and MA. The ratio  $P$  of  $P_{vcm}$  and  $P_{ma}$  is a 16th order model and the four parameters provide little freedom to place poles, but stability can be obtained with the parametrization of (7).

The structural interference between the VCM and MA can be measured by the minimum damping ratio of the pole location, defined by

$$\xi = \min_i \left\{ -\cos \left( \tan^{-1} \left( \frac{\text{imag}\{\lambda_i\}}{\text{real}\{\lambda_i\}} \right) \right) \right\}$$

where  $\lambda_i$ ,  $i = 1, \dots, 19$  are the closed-loop poles of the feedback connection of the 16th order model  $P(s)$  and the 3rd order controller  $Q(s)$ . The root-locus method provides the parameters

$$K = 161, \tau_d = 1.193 \cdot 10^{-3} \\ \tau_1 = 3.185 \cdot 10^{-3}, \tau_2 = 1.326 \cdot 10^{-4}$$

and a location of the zeros of  $G_{siso}$  where the minimum damping ration  $\xi$  was found to be approximately  $4.5 \cdot 10^{-3}$ , providing sufficient decoupling of the VCM and MA.

In the second step of the PQ-method, the common controller  $C_0$  is designed to achieve a closed-loop bandwidth of the dual-stage control system of approximately 1kHz, while maintaining amplitude and phase margins for robustness. A root-locus method provides the parameters

$$K_0 = 50, \omega_0 = 4.39 \cdot 10^3, \beta_0 = 0.5$$

and a dual-stage control system with a gain and phase margin of 16.7dB and 40 degrees respectively is obtained. The single-stage controller is designed with the same design freedom  $C_{ss}(s) = C_{vcm}(s)C_0(s)$  with  $C_{vcm}$  and  $C_0$  given in (6) and (8). Moreover, the same closed-loop bandwidth of 1kHz is used to design the single-stage controller  $C_{ss}$ . When simulating a  $1\mu\text{m}$  disturbance response, the difference between the single- and dual-stage control system can be observed from Figure 5. The dual-stage control system achieves a faster settling time despite the fact that the VCM control signal is slower.

#### 4.3 Instrumented Dual-Stage Suspension Design

In this study we built upon previous work in which experimentally obtained models for  $P_{ima}$  were used to design an inner-loop controller  $C_i$  that reduces high frequency vibrations due to windage by exploiting the flexibility of the suspension (Vestmoen Nilsen and de Callafon, 2004). The resulting instrumented controller  $C_i$  is designed as a notch filter centered around the resonance frequency of the dual-stage suspension at approximately 9kHz.

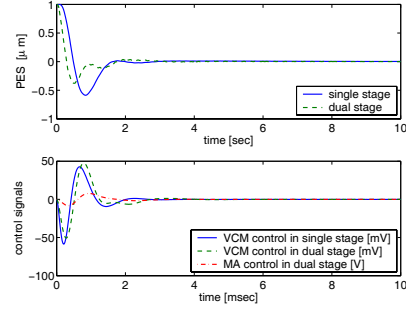


Fig. 5. Single versus dual-stage step disturbance response with PES signal in top figure and control signals in bottom figure

The change in MA dynamics due to the inner-loop controller  $C_i$  requires a redesign of the dual-stage controller. As in the previous dual-stage design, the parameters of the instrumented dual-stage actuator given by equations (6) through (9), are designed via standard root-locus techniques. The following values are obtained:

$$K = 170, \tau_d = 1.193 \cdot 10^{-3}, \\ \tau_1 = 3.185 \cdot 10^{-3}, \tau_2 = 1.333 \cdot 10^{-4} \\ K_0 = 30, \omega_0 = 4.084 \cdot 10^3, \beta_0 = 0.4$$

and indicate a controller with a larger DC-gain, but with a stronger high frequency roll-off. The larger DC-gain of the controller is due to smaller gain of the MA, as only one piezo element is used for actuation. The bandwidth of the controlled instrumented MA system is 650Hz and smaller than with the conventional dual-stage actuator at 650Hz. The gain and phase margin are 11 and 40.

The difference between the conventional dual-stage MA and the instrumented dual-stage MA with inner-loop control can be seen in Figure 6, where a simulation of a  $1\mu\text{m}$  step disturbance response is given. The results indicate a slightly larger settling time of the instrumented dual-stage controlled MA. The benefit of using an inner-loop controller and designing an outer-loop dual-stage controller becomes clear after observing the sensitivity function of the control system. Due to the inner-loop controller, the sensitivity function exhibits disturbance rejection at the location of the sway mode of the suspension. The price to be paid is a slightly smaller bandwidth of the outer-loop controller, designed by the PQ-method.

#### 4.4 Implementation results

In order to demonstrate the favorable properties of the servo design procedure proposed in this paper for an instrumented suspension with inner-loop control, the experimental setup depicted in Figure 1 was used to implement the dual-stage and inner-loop controller. The 4th order inner-loop controller is implemented using a 12bit DA/AD real-time floating point control system, where a high pass filtered ISS signal sampled at

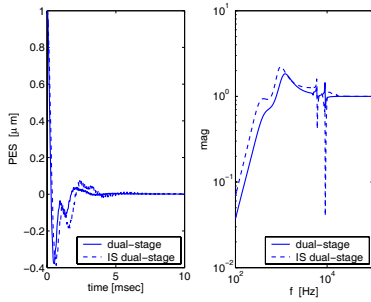


Fig. 6. Step response disturbances (left) and sensitivity function (right) of dual-stage design (solid) versus dual-stage design with inner-loop instrumented controller (dashed)

40kHz is used to ensure the reduction of windage induced vibrations of the instrumented suspension (Vestmoen Nilsen and de Callafon, 2004). To resemble the larger sampling frequency of the PES, obtained via Laser Doppler Vibrometer (LDV), the 4th order dual-stage controller is implemented using a 12 bit AD sampling at 20kHz such that the 9kHz sway mode can still be observed.

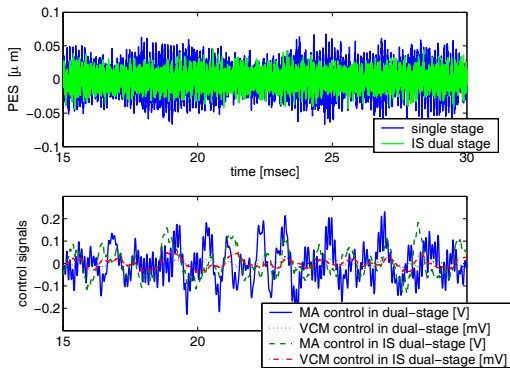


Fig. 7. Time traces of PES signal (top) and control signal from the dual-stage controller (bottom)

Referring to the top plot in Figure 7, it can be observed that the LDV measurement of the PES for the conventional dual-stage controller indicates good track following properties. However, the PES exhibits occasional bursts due to the random excitation of the highly flexible sway mode of the suspension. On the other hand, the dual-stage controller with inner-loop control shows a smaller variance of the PES due to active control of the suspension on the basis of the ISS. Residual vibrations of the suspension are controlled by the inner-loop controller, resulting in smaller PES variance and smaller control signals from the dual-stage controller. Although the dual-stage controller for the instrumented suspension brought about a decrease in the overall system bandwidth, the non-repeatable run out errors due to windage disturbances are reduced.

## 5. CONCLUSIONS

This paper introduces an explicit parametrization for a low order dual-stage controller to facilitate the PQ-method for dual-stage controller design. The parametrization gives a direct relation between the VCM and the micro-actuator controller in terms of the design freedom to place poles and zeros of the feedback control system. The dual-stage control design is applied to an instrumented suspension, where a high sampling frequency inner-loop controller is designed separately from the dual-stage controller. The procedure is demonstrated on an experimental set up to control a dual-stage instrumented suspension. Results comparing conventional versus instrumented suspensions show that higher bandwidth does not necessarily correspond to a reduction in the high frequent non repeatable run out errors.

## REFERENCES

- G.F. Franklin, J.D. Powell, and A. Emami Naeini. *Feedback Control of Dynamic Systems*. Prentice-Hall, NJ, 2002.
- Y. Li and R. Horowitz. Design and testing of track-following controllers for dual-stage servo systems with PZT actuated suspensions. *Microsystems Technologies*, 8:194–205, 2002.
- Y. Li, R. Horowitz, and R. Evans. Vibration control of a pzt actuated suspension dual-stage servo system using a pzt sensor. *IEEE Trans. on Magnetics*, 39:932–937, 2003.
- L. Ljung. *System Identification: Theory for the User (second edition)*. Prentice-Hall, Englewood Cliffs, New Jersey, USA, 1999.
- A. Mamun, I. Mareels, T.H. Lee, and A. Tay. Dual stage actuator control in hard disk drive - a review. *IEEE Trans. on Magnetics*, 2003.
- M. Rotunno and R.A. de Callafon. Comparison and design of servo controllers for dual-stage actuators in hard disk drives. *IEEE Transactions on Magnetics*, 39:2597–2599, 2003.
- S.J. Schroeck, W.C. Messner, and R.J. McNab. On compensator design for linear time invariant dual-input single-output systems. *IEEE/ASME Trans. on Mechatronics*, 6, March 2001.
- T. Suthasun, I. Mareels, and Al-Mamun A. System identification and controller design for dual actuated hard disk drive. *Control Engineering Practice*, 12:665–676, 2004.
- A.P. Teerhuis, S.J. Cools, and R.A. de Callafon. Reduction of flow induced suspension vibrations in a hard disk drive by dual stage suspension control. *IEEE Trans. On Magnetics*, 8, 2003.
- N.K. Vestmoen Nilsen and R.A. de Callafon. Control design for a piezo-electric dual-stage instrumented suspension. *Proc. 6th IASTED Int. Conference on Control and Applications*, pages 99–104, 2004.